Efficient CO_2 capture from ambient air with Amine-functionalized Mg–Al mixed metal oxide nanosheets

Xuancan Zhu[1], Tianshu Ge[1,*], Fan Yang[1], Meng Lyu[2], Chunping Chen[2], Dermot O'Hare[2], Ruzhu Wang[1,**]

1 Institute of Refrigeration and Cryogenics, Shanghai Jiao Tong University, Engineering Research Center of Solar Energy, MOE China, 800 Dongchuan Road, Shanghai, 200240, China

2 Chemistry Research Laboratory, Department of Chemistry, University of Oxford, 12 Mansfield Road, Oxford, OX1 3TA, UK.

* Corresponding author: E-mail: baby_wo@sjtu.edu.cn; Tel: +86 13916150639

** Co-corresponding author: E-mail: rzwang@sjtu.edu.cn; Tel: +86 15800967634

Abstract

In this work, we report a new family of class 1 adsorbents for direct air capture of CO_2 prepared by loading branched poly(ethylenimine) (PEI) into Mg-Al-CO_3 layered double hydroxide-derived mixed metal oxides (MMOs), which exhibit unexpectedly large adsorption capacities, fast kinetics, and high stability. First, the bulk phase MMO precursors are successfully exfoliated into nanosheets with the plate size of approximate 20 nm by reduced Mg/Al ratios and also via aqueous miscible organic solvent treatment. Upon vacuum heating, the MMO layers are self-assembled into spherically shaped particles with abundant slit-like mesopores, large surface areas, and broad pore distribution. This ideal nanostructure leads to the uniform distribution of the impregnated PEI, and thus, it creates optimal accessibility for CO_2 molecules to the exposed strong adsorption sites under ultradilute conditions. At high PEI loading ratios, PEI starts to cover the MMO framework but the porous structure is still present and no significant decrease in amine efficiency is observed. Remarkably, the 67 wt.% PEI-impregnated $Mg_{0.55}Al$-O MMO reaches the total CO_2 adsorption capacity of 2.27 mmol/g and the fast adsorption rate of 1.1 mmol/g·h within 90 min at 25 °C under 0.4 mbar CO_2. In addition, the defect-abundant MMO layers provide strong electrostatic attraction to the attached polyamines, making the hybrid adsorbents highly robust during thermal regeneration up to 300 °C. Enhanced CO_2 adsorption capacity and stability are observed during multi-cycle tests in the presence of moisture attributed to the changes in the adsorption mechanism and circumventing the CO_2-induced deactivation, thus facilitating the use of steam stripping to concentrate the CO_2 desorbed

from amine-functionalized MMOs.

Keywords

Direct air capture; Amine-functionalized adsorbent; Mixed metal oxide; Poly(ethylenimine); Thermal stability; Hydrothermal stability

Introduction

Direct air capture (DAC) is a type of negative emissions technology that can be used to extract CO_2 from the atmosphere via absorption or adsorption. Compared to conventional CO_2 capture technologies that are used to remove CO_2 from large point sources, DAC is advantageous because it could be used for distributed CO_2 emissions, it presents no location restrictions for the placement of the capture facilities, and its performance is not affected by contaminants, such as SO_x, NO_x, and heavy metals.[1] Furthermore, when DAC is coupled with CO_2 chemical conversion technologies it could provide carbon sources for the production of fuels, biofuels, pharmaceuticals, high-value chemicals, greenhouse feeding nutrients, and agricultural.[2–6] Early DAC systems have used aqueous alkali or alkali-earth hydroxides, which extracted CO_2 via causticization or alternative causticization.[7,8] However, the high energy demands for their thermal regeneration, large amounts of water loss, and use of pure O_2 have limited their implementation, and therefore, researchers changed their focus to adsorbent-based systems.[9,10]

When selecting appropriate adsorbents for DAC one should comprehensively consider their cost, adsorption capacity, kinetics, multi-cycle stability, and selectively. In addition, the binding force between CO_2 and adsorption sites should be strong enough because the CO_2 in the atmosphere is extremely dilute (approximately 400 ppm, which is only 1/350 of the CO_2 concentration in flue gas). Therefore, solid-supported amines are suitable DAC adsorbents owing to their chemisorption properties and low regeneration temperatures (commonly below 120 °C).[11,12] Supported amines react with

CO_2 to form ammonium carbamate under anhydrous conditions[13,14] or ammonium carbonate/bicarbonate in the presence of moisture.[15] Amines could be physically loaded (class 1), covalently tethered (class 2), or *in situ* polymerized (class 3) onto solid supports.[16] Recently, class 1 adsorbents, which do not involve chemical reactions with the mesostructured supports have become highly attractive for commercial-scale DAC applications because of their low cost and relatively large CO_2 adsorption capacities under ultradilute conditions.[17–25] Low molecular weight primary amine-rich branched poly(ethylenimine) (PEI) is commonly used for class 1 adsorbents, as smaller amines lead to considerable evaporation and amine loss,[26] whereas high molecular weight PEI could hinder the diffusion of CO_2 into the porous matrix.[27]

Although it is believed that amine loading mainly determines the CO_2 uptake of solid-supported amine materials, the textural properties and surface microstructure of the support could change the morphology of amines within the support and the gas-surface interaction, and consequently, could significantly affect their overall CO_2 capture efficiency. Silica materials, such as commercial silica,[28] fumed silica,[27,29] SBA-15,[30–35] silica fiber,[17] pore-expanded MCM-41 (PE-MCM-41),[36] and mesocellular foam (MCF),[37] have been widely studied for DAC applications owing to their large surface areas, high pore volumes, and narrow pore size distributions. Despite exhibiting promising adsorption capacities and amine efficiencies, PEI/silica composites present kinetics and thermal stability drawbacks. Choi et al.[28] reported that 45 wt.% PEI-impregnated commercial silica reached the high CO_2 uptake of 2.36 mmol/g during the first adsorption cycle (400 ppm CO_2/Ar, 25 °C), but the long adsorption half-time of

309 min was needed and 30% of the adsorption capacity was lost after only four cycles. Another evidence is that the maximum CO_2 uptake of highly amine-loaded PEI/silica was achieved at elevated temperatures to overcome the kinetic limitation.[27] The chemical (oxidative degradation and CO_2-induced deactivation) and hydrothermal stabilities of PEI/silica composites are also challenging, and this is particularly important when steam stripping is used in DAC systems to produce concentrated CO_2 streams.[38]

To address the above-mentioned drawbacks, it is necessary to design support materials with suitable morphology, strong affinity to polyamines, and high thermal and hydrothermal resistance. It has been reported that both the stability and CO_2 adsorption kinetics of PEI/silica composites could be improved via the addition of 3-aminopropyltriethoxysilane and tetraethyl orthotitanate, because these compounds strengthen the bonding between PEI and the surface of silica.[39] The co-addition of polyethylene glycol to PEI/silica composites could also increase their air capture performance owing to the improved arrangement of PEI with scattered aggregates.[34] Support modification is another strategy that could be used to improve the CO_2 adsorption efficiency of PEI/silica composites under ultradilute streams. Kuwahara et al.[30,31] demonstrated that incorporating heteroatoms into SBA-15 changed the acid/base properties of the support, and thus increased not only the CO_2 uptake but also the regenerability and thermal stability of the adsorbent. However, a later study indicated that the improved CO_2 adsorption properties were more likely related to the changes in texture of the supports (larger pore volume, pore size, and less microporosity).[32] Sayari

et al.[36] determined that excellent amine efficiency and stability could be achieved using PE-MCM-41 with abundant surface cetyltrimethylammonium ($CTMA^+$) cations. They concluded that the $CTMA^+$ layer effectively changed the dispersion of PEI on the surface of silica and thus increased amine accessibility. Several researchers used non-silica supports, such as mesoporous carbon and γ-alumina. The use of mesoporous carbon frameworks and additives promoted both pore and amine diffusion, which led to remarkable kinetics and stability at high PEI loadings.[40] PEI-loaded alumina also exhibited high stability under steam striping, but its CO_2 adsorption capacity was lower than that of PEI/silica composites.[41,42]

In this paper, we report a new family of class 1 adsorbents for DAC; these adsorbents were obtained by loading PEI into layered double hydroxide (LDH)-derived mixed metal oxides (MMOs), which exhibited unexpectedly large adsorption capacity, fast kinetics, and high stability. LDHs are two-dimensional layered materials comprising brucite-like layers separated by charge-compensating anions and interlayered water, and their general formula is $[M_x^{2+}M^{3+}(OH)_{2x+2}]^+(A^{n-})_{1/n}\cdot mH_2O$. Each metal cation is coordinated with six –OH groups, which are edge-sharing, to form infinite 2D sheets. Stacked bulk LDHs could be exfoliated into small plates using the aqueous miscible organic solvent treatment (AMOST) method, which was recently developed by O'Hare's group.[43,44] Their large specific surface area, ultrathin nanosheets, and tunable metal cations render exfoliated LDHs usable for catalysts, adsorption, biomedicine, water treatment, and electrochemistry.[45] Upon thermal treatment, LDHs undergo dehydration, dihydroxylation, and decarbonation processes and form MMOs

with abundant surface defects.[46] The use of MMOs as supports allowed the development of ideal CO_2 diffusion channels through the slit-shaped mesopores formed by the exfoliated nanosheets, and the extra pores derived from the release of gas molecules, such as CO_2 and H_2O, during calcination. Impregnated polyamines are supposed to disperse well on defect-abundant MMO layers owing to their strong electrostatic attraction even in the absence of additives. Furthermore, the morphology and chemical properties of MMOs could be adjusted by changing the type and relative ratios of divalent and trivalent metal cations, which facilitated the optimization of the CO_2 capture efficiency of the PEI/MMO composites.

Results and discussion

Two types of Mg_xAl-CO_3 LDH (x = 2, 3) were successfully prepared using the AMOST method, and the metal contents of the samples were determined using inductively coupled plasma optical emission spectrometry (ICP-OES) tests (Table S1, Supporting Information). A compound using Mg:Al in the ratio of 0.55 was also prepared ($Mg_{0.55}Al$-CO_3) (Table S1). All samples exhibited exfoliated morphologies with flower-like structures and slit-shaped mesopores (Figure 1). The size of the sample nanosheets could be adjusted from 200 to 20 nm by changing x owing to the increase in the content of Al^{3+} ions introducing more defects into the brucite-like MgO structure.[47] The typical LDH patterns of the samples were confirmed using X-ray diffraction (XRD) analysis, and the results are presented in Figure S1a. The XRD pattern of $Mg_{0.55}Al$-CO_3 suggested that it is a mixed phase of LDH and Al-containing impurities (*e.g.* $Al(OH)_3$). As x decreased the (003) and (006) peaks shifted toward larger angles, which indicated

that the interlayer spacing was shortened owing to the stronger electrostatic interactions between the positively charged layers. After calcination at 450 °C for 5 h, all samples were transformed into MMOs (denoted as Mg_xAl-O), and only weak XRD peaks could be observed between the MgO and the Al_2O_3 ones (Figure S1b). The thermogravimetric analysis (TGA) and derivative thermogravimetry analyses data (Figure S2) revealed differences between the bulk MMO precursors and acetone-washed ones; namely, the temperatures of the weight loss stages of the treated precursors were lower than those of the bulk precursors because the treated nanosheets exfoliated easier.[44] The N_2 adsorption–desorption isotherms at 77 K and the DFT pore size distributions of the supports determined using the density functional theory are illustrated in Figure S3, whereas the calculated textural properties are listed in Table S2. Compared to SBA-15, which featured uniform mesopores approximately 7.4 nm in size, both MMOs and γ-Al_2O_3 exhibited much lower surface areas but comparable pore volume, broader pore size distributions, and higher average pore diameters, and thus the diffusion of CO_2 was promoted via the loading of high amounts of PEI.

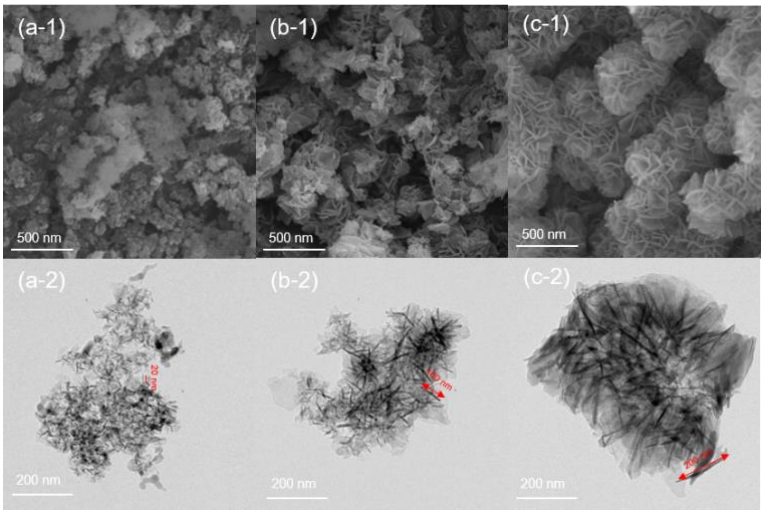

Figure 1. Scanning and transmission electron microscopy images of Mg_xAl-CO_3

mixed metal oxide precursors synthesized using the aqueous miscible organic solvent treatment method; (a) x = 0.55, (b) x = 2, and (c) x = 3.

The screening results of the CO_2 adsorption isotherm of the 33 wt.% PEI-impregnated samples (denoted as PEI33/support) at 25 °C (Figure 2a) revealed the effect of the support on amine efficiency. The CO_2 adsorption capacity of PEI33/γ-Al_2O_3 was slightly lower than that of PEI33/SBA-15. By contrast, the capacity of PEI33/$Mg_{0.55}$Al-O at 0.4 mbar (1.080 mmol/g) was comparable to that of PEI33/SBA-15, which suggested that MMOs could be used as candidates for PEI supports. The low capacity of PEI33/MgO was attributed to the small surface area and pore volume of the MgO support (Table S2). Interestingly, the capacities of PEI33/Mg_2Al-O and PEI33/Mg_3Al-O were unsatisfactory, despite their supports presenting surface areas and pore distributions similar to that of PEI33/$Mg_{0.55}$Al-O. It was therefore assumed that the morphology of $Mg_{0.55}$Al-O which featured small plate sizes could play a critical role in enhancing the adsorption efficiency of the impregnated PEI. Subsequently, the effect of the PEI loading (0, 33, 50, and 67 wt.%) on SBA-15 and $Mg_{0.55}$Al-O was studied (Figure 2b and Figure S4, respectively). The CO_2 adsorption capacity of the prepared PEI/$Mg_{0.55}$Al-O at 0.4 mbar increased linearly as the PEI loading ratio increased, whereas the amine efficiency of PEI/SBA-15 started to decrease at PEI loadings that exceeded 50 wt.%. Remarkably, the CO_2 adsorption capacity of PEI67/$Mg_{0.55}$Al-O reached 2.272 mmol/g, which was 18% higher than that of PEI67/SBA-15. In addition, the near zero initial capacities of the supports indicated that almost all the CO_2 adsorption sites under ultradilute conditions were attributed to the chemisorbed PEI.

Next, we investigated the performance of PEI67/$Mg_{0.55}$Al-O at higher adsorption temperatures, and the results indicated that the prepared sample was able to adsorb a significant amount of CO_2 at 0.4 mbar up to 65 °C (Figure 2c). The heat of adsorption of PEI67/$Mg_{0.55}$Al-O was evaluated to be 75.3 kJ/mol using the Clausius−Clapeyron equation (Figure S5), and this was larger than that reported for branched PEI/SBA-15 (which is typically 50–60 kJ/mol).[48]

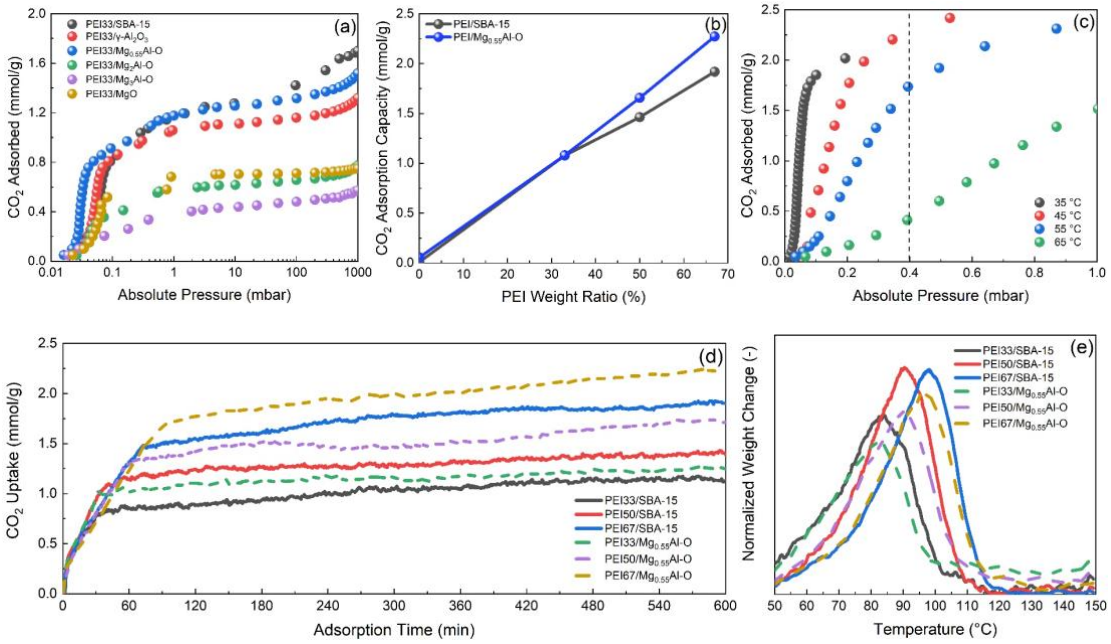

Figure 2. Characterization of CO_2 adsorption performance of poly(ethylenimine) (PEI)-based adsorbents in ultradilute conditions: (a) screening of CO_2 adsorption isotherms at 25 °C for 33 wt.% PEI-impregnated supports, (b) effect of PEI weight ratios for PEI impregnated SBA-15 and $Mg_{0.55}$Al-O, (c) CO_2 adsorption isotherms of PEI67/$Mg_{0.55}$Al-O at different adsorption temperatures, (d) CO_2 adsorption kinetics of PEI-impregnated SBA-15 and $Mg_{0.55}$Al-O at 25 °C under 400 ppm CO_2 in N_2, and (e) temperature programmed desorption of PEI-impregnated SBA-15 and $Mg_{0.55}$Al-O.

The CO_2 adsorption kinetics of the PEI/SBA-15 and PEI/$Mg_{0.55}$Al-O with different PEI loadings were compared using TGA tests at 25 °C under 400 ppm CO_2 in N_2 atmosphere (Figure 2d). All samples exhibited fast initial CO_2 adsorption followed by a slow diffusion-controlled stage during the remaining duration of the test (600 min). The fast uptakes of PEI/$Mg_{0.55}$Al-O during the first stage, which was surface reaction rate-limited, were larger than that of PEI/SBA-15 for all the three analyzed PEI loadings. The temperature programmed desorption (TPD) results in Figure 2e further revealed that more strong adsorption sites existed on PEI/$Mg_{0.55}$Al-O than on PEI/SBA-15, which required higher temperatures of up to 150 °C to be fully regenerated. Therefore, it was concluded that the use of $Mg_{0.55}$Al-O promoted the uniform distribution of the impregnated PEI on the surface of the support, which facilitated the accessibility of CO_2 molecules to the exposed strong adsorption sites and promoted the CO_2 adsorption kinetics in ultradilute conditions.

The morphology and PEI distributions of PEI/$Mg_{0.55}$Al-O were studied to further understand the enhanced CO_2 capacities and kinetics of PEI-impregnated MMOs (Figure 3). After vacuum thermal treatment, the exfoliated $Mg_{0.55}$Al-O nanosheets aggregated into spherical particles approximately 100 nm in diameter. At the low PEI loading of 33 wt.%, the impregnated PEI preferentially attached to the sides of the MMO layers, which led to the formation of thicker and larger nanosheets and the gradual increase in particle size. Abundant slit-like channels for CO_2 diffusion remained when the PEI loading reached 50 wt.%. At higher PEI loadings, which exceeded the pore volume of the support, the MMO nanosheets started to be covered by PEI.

However, the stacked PEI still presented porous morphology owing to the use of $Mg_{0.55}Al$-O as the basic framework. The energy dispersive spectroscopy (EDS) results indicated that the impregnated PEI was distributed uniformly in the PEI/$Mg_{0.55}Al$-O composites with different PEI loadings. The results of the N_2 adsorption–desorption tests, which were conducted at 77 K, provided further insight into the changes in the structure of the supports after PEI impregnation (Figure 4 and Table S3). Despite its initial surface area being larger than that of SBA-15, $Mg_{0.55}Al$-O effectively prevented pore blockage and presented more reasonable pore size distributions, larger surface area, and pore volume for CO_2 diffusion after PEI loading.

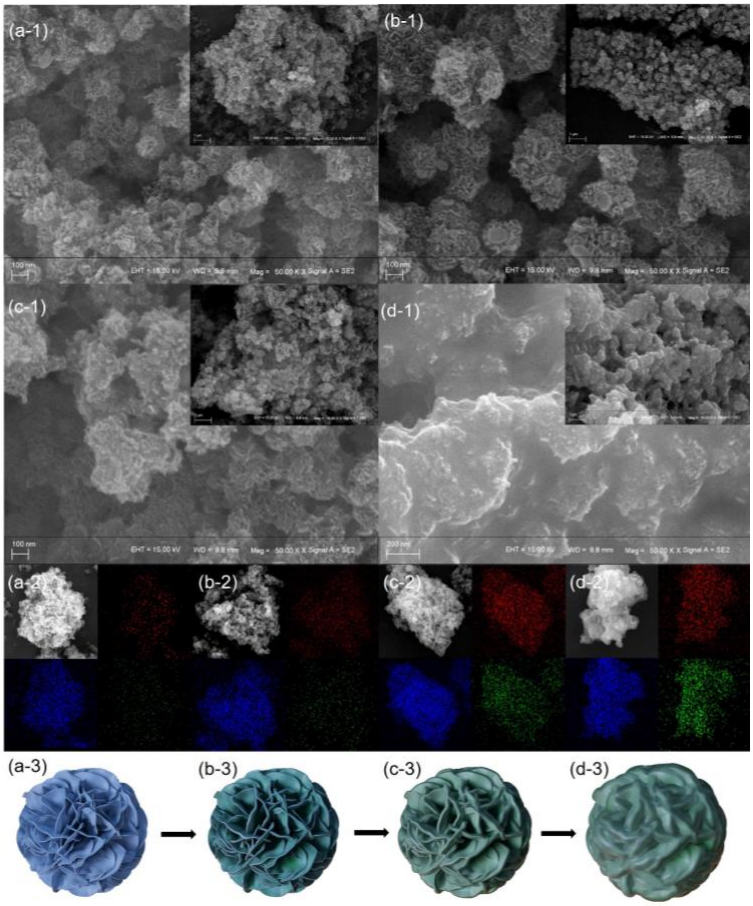

Figure 3. Scanning electron microscopy images and energy dispersive X-ray spectroscopy (EDS) results of (a) $Mg_{0.55}Al$-O, (b) PEI33/$Mg_{0.55}Al$-O, (c)

PEI50/$Mg_{0.55}$Al-O, and (d) PEI67/$Mg_{0.55}$Al-O. The red, blue, and green spots in the EDS scans represent Mg, Al, and N, respectively.

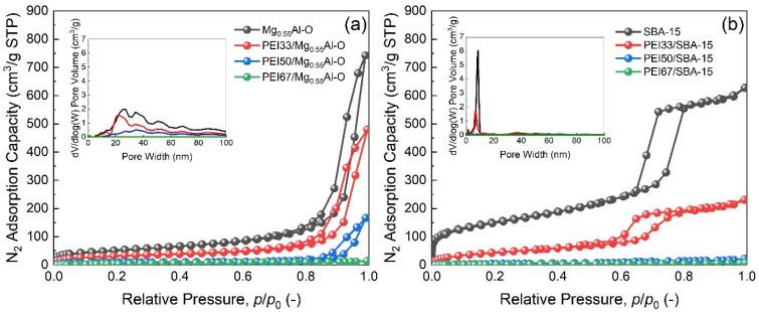

Figure 4. N_2 adsorption-desorption isotherms at 77 K and density functional theory pore distributions of PEI-impregnated (a) $Mg_{0.55}$Al-O and (b) SBA-15 with different PEI loadings.

Amine-functionalized CO_2 adsorbents, particularly class 1 adsorbents without aminosilanes linking, commonly face stability problems.[38] However, the thermal decomposition results depicted in Figure 5a and Figure S6 provided strong evidence for the interactions between the impregnated amines and supports. Two weight loss peaks, which were 350 °C apart, were present in the curve of PEI/SBA-15. The low-temperature peak was related to the decomposition of the PEI dispersed in the pores of SBA-15 and the high-temperature peak was ascribed to the breaking of the hydrogen bonds between the remaining amine and silanols on the support.[39] Both peaks shifted toward higher temperatures as the PEI loadings increased, and this was attributed to the agglomeration of PEI into larger particles. In contrast, only the peak above 350 °C was observed in the curves of all PEI/$Mg_{0.55}$Al-O samples and the peak temperature did not change significantly, which suggested the presence of strong interactions between PEI and $Mg_{0.55}$Al-O. It was also determined that the CO_2 adsorption capacity of

PEI67/SBA-15 rapidly decreased after it underwent desorption above 200 °C, whereas the adsorption capacity of PEI67/$Mg_{0.55}$Al-O did not decrease until the temperature reached 300 °C (Figure 5b). Moreover, a slight increase in the CO_2 adsorption capacity of PEI67/$Mg_{0.55}$Al-O was observed at higher desorption temperatures, which could be ascribed to the enhanced kinetics owing to the presence of the optimized CO_2 diffusion channel and increased surface area after moving the weakly attached PEIs (Figure S7). It has been demonstrated that coordinatively unsaturated oxygens or metals were created via the insertion of Al^{3+} ions into MMOs with periclase MgO lattice or the escape of Al atoms from layers during calcination, and their density increased as the lateral size of the MMO layers decreased.[49,50] Therefore, the defect-abundant $Mg_{0.55}$Al-O nanosheets were supposed to facilitate the strong electrostatic attractions between the impregnated PEI and MMO layers, which rendered the PEI/$Mg_{0.55}$Al-O composites thermally robust (Figure 5c).

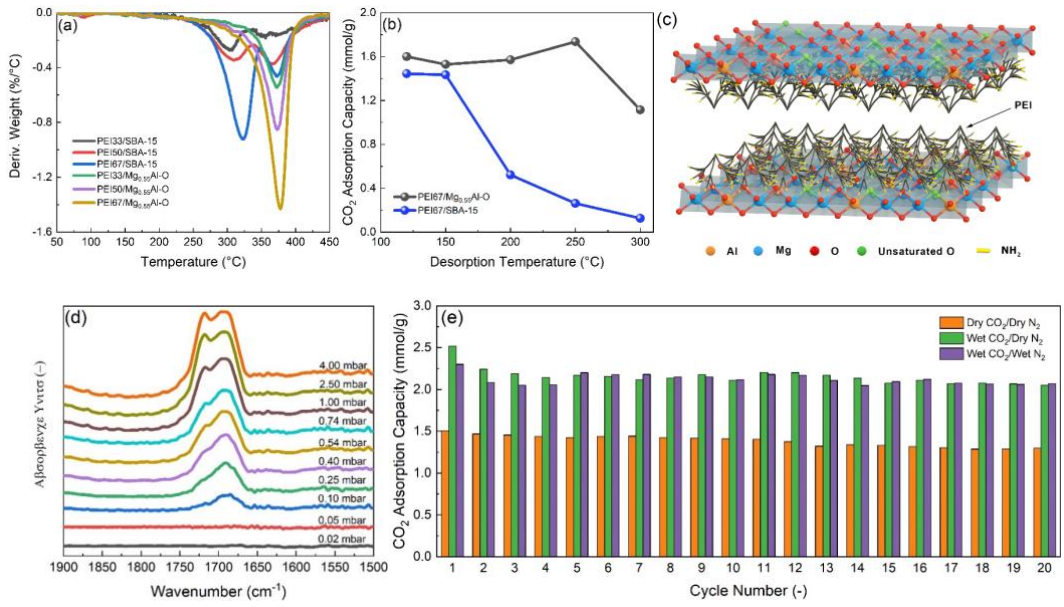

Figure 5. Stability of poly(ethylenimine) (PEI)-impregnated samples under direct air capture conditions: (a) thermal stability from 50 to 450 °C at heating rate of

5 °C/min under N_2 flow, (b) CO_2 uptake in 2 h at 400 ppm CO_2 and 25 °C after desorption at different temperatures, (c) schematic diagram of PEI/MMOs structure (MMOs denotes layered double hydroxide-derived mixed metal oxides), (d) *in situ* infrared spectroscopy for the CO_2 adsorption of PEI67/$Mg_{0.55}$Al-O at 25 °C, and (e) cyclic stability of PEI67/$Mg_{0.55}$Al-O with 2 h adsorption at 25 °C followed by 1 h desorption at 120 °C.

To further verify the stability of PEI67/$Mg_{0.55}$Al-O, cyclic breakthrough tests were conducted using a home-made fixed bed microreactor system (Figure S8). The capacity of PEI67/$Mg_{0.55}$Al-O during at least 20 cycles that consisted of 2 h adsorption at 25 °C under 400 ppm CO_2 in the absence of moisture followed by 1 h desorption at 120 °C under pure N_2 atmosphere was determined to be stable; the slight decrease in performance of 0.01 mmol/g per cycle was ascribed to the composite coming into contact with highly concentrated CO_2 during the regeneration step via the formation of urea linkages.[51] Interestingly, the CO_2 adsorption capacity of PEI67/$Mg_{0.55}$Al-O increased by 50% for wet CO_2 when the inlet gas was passed through a scrubbing bottle (Figure S9). The supported amines formed ammonium carbamate when exposed to a maximum of 0.5 mol of CO_2/mol of N under dry conditions after the adsorption of CO_2, which was confirmed using the *in situ* Fourier-transform infrared spectroscopy (FTIR) spectra in Figure 5d. However, it was reported that the CO_2 adsorption mechanism was changed to the formation of ammonium carbonate/bicarbonate when the supported amines were exposed to a maximum of 0.5 mol of CO_2/mol of N in the presence of moisture.[15] The results depicted in Figure 5e also suggested that $Mg_{0.55}$Al-O efficiently

prevented blocking the access of amine via water oversaturation at high PEI loadings, which has been commonly reported for silica-based materials.[29] In addition, there have been no noticeable changes in the performance of the proposed PEI/MMO composites when wet N_2 was used during thermal regeneration, which indicated that steam stripping could be a possible strategy for concentrating the desorbed CO_2.

Conclusions

A new family of PEI-functionalized Mg-Al-CO_3 MMO class 1 adsorbents was proposed in this work. The low Mg/Al ratios of Mg_xAl-CO_3 and use of the AMOST method lead to the exfoliation of the MMO precursors into nanosheets with plate sizes in the range of 20–200 nm, which self-assembled into spherical particles upon thermal treatment. The impregnated polyamines dispersed uniformly on the surface of the MMO nanosheets, and thus, they created optimal accessibility for the CO_2 molecules to the exposed strong adsorption sites under ultradilute conditions. At high PEI loading ratios of up to 67 wt.%, the polyamines started to cover the MMO frameworks but the porous structure was still maintained and their amine efficiency was not significantly decreased. The proposed PEI/MMO composites exhibited higher CO_2 adsorption capacity and better kinetics than PEI/SBA-15 owing to the ideal morphologies and nanostructures of their supports. In addition, the defect-abundant MMO layers provide strong electrostatic attraction to the attached polyamines, which contributed to the robustness of the hybrid adsorbents for at least 20 cycles in the absence and presence of moisture. Overall, the low cost, facile fabrication, and promising CO_2 capacities, kinetics, and thermal and hydrothermal stabilities rendered amine-functionalized

MMOs attractive for scalable CO_2 capture applications under ultradilute conditions.

Experimental section

Synthesis of MMOs

We synthesized MMO precursors using co-precipitation combined with AMOST, and the detailed synthesis procedure has been described in one of our previously published papers.[47] All chemicals used for the synthesis were of analytical purity. Typically, 1 M metal precursor ($Mg(NO_3)_2 \cdot 6H_2O$ and $Al(NO_3)_3 \cdot 9H_2O$) solution was slowly added to an equal amount of 0.5 M Na_2CO_3 solution under vigorous stirring, and the pH was adjusted to 10.0 ± 0.1 by adding NaOH solution to the mixture. The mixture was then aged at 25 °C for 16 h followed by adequate flushing with deionized water. The key step for the AMOST method is the use of aqueous miscible organic (AMO) solvents to rinse and re-disperse the wet sample cake before it is dried. This process was determined to be efficient for the removal of the interlayered water. The AMO solvent (acetone in this study) was then volatilized via overnight vacuum drying to facilitate the exfoliation of the sample nanosheets. The MMOs were obtained via the vacuum calcination at 450 °C for 5 h. The prepared MMO precursors and MMOs were denoted as $Mg_xAl\text{-}CO_3$ and $Mg_xAl\text{-}O$, respectively, where x is the Mg/Al molar ratio.

Preparation of adsorbents

The PEI-based adsorbents were synthesized via wet impregnation. Typically, the MMOs were vacuum dried overnight at 100 °C to remove any adsorbed species. A given amount of branched PEI (Alfa Aesar, $M_w \approx 600$) was dispersed into 20 mL methanol. After the dispersion reached equilibrium, 0.5 g dried support was added to it

and the mixture was stirred at 25 °C under N_2 protection for 3 h. Methanol was subsequently removed via rotatory evaporation followed by vacuum drying the resulting powder at 60 °C for at least 12 h. Prior to analysis, the samples were vacuum-stored in vials under atmosphere temperature. For comparison, commercially available mesoporous materials, such as SBA-15 (which was purchased from Nanjing XFNANO Materials Tech Co., Ltd), γ-Al_2O_3 (which was procured from D-chem), and light MgO (which was acquired from Sinopharm Chemical Reagent Co., Ltd) were also used as supports. The prepared adsorbents were denoted as PEI*y*/support, where *y* represents the weight ratio of PEI in the PEI/support composite.

Material characterization

The crystal structure of the samples was characterized using a MiniFlex600 (Rigaku) powder XRD instrument with Cu K_α radiation at 40 kV and 15 mA in the 2θ range of 5° to 90°. The morphologies and element distributions of the samples were observed using a MAIA3 (TESCAN) scanning electron microscopy (SEM) apparatus equipped with an EDS detector and a Talos L120C G2 (Thermo Scientific) transmission electron microscope. Prior to the SEM experiments, the powdered samples were sprayed with Au for 30 s. The Mg/Al ratios of the MMO precursors were determined using an iCAP-7600 (Thermo-Fisher) ICP-OES system. The textural properties of the samples were measured via N_2 adsorption at 77 K using an ASAP 2460 (Micromeritics) surface area and porosity analyzer, and the surface area/average pore diameters and pore volumes were evaluated using the Brunauer–Emmett–Teller and Barrett–Joyner–Halenda desorption methods, respectively. The MMO precursors were thermally decomposed in

363 the temperature range of 50 to 800 °C using a Q5000IR (TA Instruments) TGA
364 instrument at the heating rate of 10 °C/min.

365 **CO_2 adsorption measurement**

366 CO_2 adsorption isotherms in the pressure range of 0−1 bar were acquired using
367 volumetric methods utilizing an ASAP2020 (Micromeritics) surface area and porosity
368 analyzer. Data points were collected after the pressure change was lower than 0.01%
369 over 5 s. The temperature of the samples (25−65 °C) was controlled using a circulator
370 bath. Before each test, samples were vacuum degassed at 100 °C for 5 h.

371 CO_2 adsorption kinetics and TPD experiments were conducted using a STA449F3
372 (Netzsch) TGA instrument. Buoyancy effects were corrected and the flow rate of 100
373 mL/min was used for all experiments. Approximately 10 mg of each sample was pre-
374 activated under high purity N_2 flow at 120 °C for 1 h. For the kinetics test, the
375 temperature was reduced to 25 °C and the purge gas was switched to 400 ppm CO_2 in
376 N_2 for 12 h. For the TPD test, the CO_2-saturated adsorbents were heated from 25 to
377 450 °C under N_2 flow at the heating rate of 5 °C/min.

378 Stability tests were conducted using a home-made fixed bed, and the details of the
379 experimental set-up are shared in the Supporting Information. Typically, 0.8 g samples
380 were loaded into a stainless-steel tube (inner diameter of 6 mm), and were alternately
381 used for adsorption at 25 °C under 400 ppm CO_2 in N_2 for 2 h followed by desorption
382 at 120 °C under pure N_2 for 1 h. Approximately 3% moisture was added to the gases by
383 passing them through a scrubbing bottle. The CO_2 content of the tail gas after drying
384 using a $CaCl_2$-filled tube was determined using an THA100S non-dispersive infrared

analyzer (0−600 ppm, ±2% full scale).

CO_2 adsorption mechanism measurement

In situ FTIR tests in the range of 4000 to 400 cm^{-1} were performed using a Bruker Tensor 27 (Bruker Optik) analyzer at the resolution of 4 cm^{-1}; 32 scans were performed for each sample. Powdered samples were pressed into 12 mg/cm^2 thick wafers, and then were loaded into a home-made stainless-steel cell with KBr windows. Prior to analysis, the samples were electrically heated to 120 °C for 1 h under vacuum to remove any adsorbed species. After cooling to 25 °C, CO_2 was step-by-step added to the sample cell using a quantitative loop, and the FTIR spectra were recorded at 30 min intervals for each pressure point.

Acknowledgement

This research was financed by National Key R&D Program of China (Grant No. 2017YFB0603702) and National Postdoctoral Program for Innovative Talent (BX20190198). Tianjin Xianquan Co., LTD is acknowledged for providing *in situ* FTIR testing services. M. Lyu acknowledges the Chinese Scholarship Council (CSC) for funding. C. Chen would like to thank SCG Chemicals Co., Ltd. (Thailand) for funding.

Reference

1. Sanz-Pérez, E. S.; Murdock, C. R.; Didas, S. A.; Jones, C. W., Direct Capture of CO_2 from Ambient Air. *Chem. Rev.* **2016,** *116* (19), 11840-11876.
2. Nikulshina, V.; Hirsch, D.; Mazzotti, M.; Steinfeld, A., CO_2 Capture From Air and Co-production of H_2 via the $Ca(OH)_2$–$CaCO_3$ Cycle Using Concentrated Solar Power–Thermodynamic Analysis. *Energy* **2006,** *31* (12), 1715-1725.
3. Veselovskaya, J. V.; Parunin, P. D.; Netskina, O. V.; Kibis, L. S.; Lysikov, A. I.; Okunev, A. G., Catalytic Methanation of Carbon Dioxide Captured from Ambient Air. *Energy* **2018,** *159*, 766-773.
4. Takeda, Y.; Okumura, S.; Tone, S.; Sasaki, I.; Minakata, S., Cyclizative Atmospheric CO_2 Fixation by Unsaturated Amines with t-BuOI Leading to Cyclic Carbamates. *Org. Lett.* **2012,** *14* (18), 4874-4877.
5. Rodríguez-Mosqueda, R.; Bramer, E. A.; Brem, G., CO_2 Capture from Ambient Air Using Hydrated Na_2CO_3 Supported on Activated Carbon Honeycombs with Application to CO_2 Enrichment in Greenhouses. *Chem. Eng. Sci.* **2018,** *189*, 114-122.
6. Rodríguez-Mosqueda, R.; Rutgers, J.; Bramer, E. A.; Brem, G., Low Temperature Water Vapor Pressure Swing for the Regeneration of Adsorbents for CO_2 Enrichment in Greenhouses via Direct Air Capture. *J. CO2 Util.* **2019,** *29*, 65-73.
7. Nikulshina, V.; Gálvez, M. E.; Steinfeld, A., Kinetic Analysis of the Carbonation Reactions for the Capture of CO_2 from Air via the $Ca(OH)_2$–$CaCO_3$–CaO Solar Thermochemical Cycle. *Chem. Eng. J.* **2007,** *129* (1), 75-83.
8. Stolaroff, J. K.; Keith, D. W.; Lowry, G. V., Carbon Dioxide Capture from Atmospheric Air Using Sodium Hydroxide Spray. *Environ. Sci. Technol.* **2008,** *42* (8), 2728-2735.
9. Shi, X.; Xiao, H.; Azarabadi, H.; Song, J.; Wu, X.; Chen, X.; Lackner, K. S., Sorbents for Direct Capture of CO_2 from Ambient Air. *Angew. Chem. Int. Edit.* **2019,** doi:10.1002/anie.201906756
10. Yang, M.; Ma, C.; Xu, M.; Wang, S.; Xu, L., Recent Advances in CO_2 Adsorption from Air: a Review. *Curr. Pollut. Rep.* **2019,** *5* (4), 272-293.
11. Didas, S. A.; Choi, S.; Chaikittisilp, W.; Jones, C. W., Amine–Oxide Hybrid Materials for CO_2 Capture from Ambient Air. *Accounts Chem. Res.* **2015,** *48* (10), 2680-2687.
12. Darunte, L. A.; Walton, K. S.; Sholl, D. S.; Jones, C. W., CO_2 Capture via Adsorption in Amine-Functionalized Sorbents. *Curr. Opin. Chem. Eng.* **2016,** *12*, 82-90.
13. Caplow, M., Kinetics of Carbamate Formation and Breakdown. *J. Am. Chem. Soc.* **1968,** *90* (24), 6795-6803.
14. Danckwerts, P. V., The Reaction of CO_2 with Ethanolamines. *Chem. Eng. Sci.* **1979,** *34* (4), 443-446.
15. Yang, Z.; He, L.; Zhao, Y.; Li, B.; Yu, B., CO_2 Capture and Activation by Superbase/Polyethylene Glycol and Its Subsequent Conversion. *Energ. Environ. Sci.* **2011,** *4* (10), 3971-3975.
16. Choi, S.; Drese, J. H.; Eisenberger, P. M.; Jones, C. W., Application of Amine-Tethered Solid Sorbents for Direct CO_2 Capture from the Ambient Air. *Environ. Sci. Technol.* **2011,** *45* (6), 2420-2427.
17. Sujan, A. R.; Pang, S. H.; Zhu, G.; Jones, C. W.; Lively, R. P., Direct CO_2 Capture from Air using Poly(ethylenimine)-Loaded Polymer/Silica Fiber Sorbents. *Acs Sustain. Chem. Eng.* **2019,** *7* (5), 5264-5273.
18. Krekel, D.; Samsun, R. C.; Peters, R.; Stolten, D., The Separation of CO_2 from Ambient Air – A Techno-Economic Assessment. *Appl. Energ.* **2018,** *218*, 361-381.
19. Vázquez, F. V.; Koponen, J.; Ruuskanen, V.; Bajamundi, C.; Kosonen, A.; Simell, P.; Ahola, J.;

Frilund, C.; Elfving, J.; Reinikainen, M.; Heikkinen, N.; Kauppinen, J.; Piermartini, P., Power-to-X Technology Using Renewable Electricity and Carbon Dioxide from Ambient Air: SOLETAIR Proof-of-Concept and Improved Process Concept. *J. CO2 Util.* **2018,** *28*, 235-246.

20. Azarabadi, H.; Lackner, K. S., A Sorbent-Focused Techno-Economic Analysis of Direct Air Capture. *Appl. Energ.* **2019,** *250*, 959-975.

21. Breyer, C.; Fasihi, M.; Bajamundi, C.; Creutzig, F., Direct Air Capture of CO_2: A Key Technology for Ambitious Climate Change Mitigation. *Joule* **2019,** *3* (9), 2053-2057.

22. E. Bajamundi, C. J.; Koponen, J.; Ruuskanen, V.; Elfving, J.; Kosonen, A.; Kauppinen, J.; Ahola, J., Capturing CO_2 from air: Technical performance and process control improvement. *J. CO2 Util.* **2019,** *30*, 232-239.

23. Fasihi, M.; Efimova, O.; Breyer, C., Techno-Economic Assessment of CO_2 Direct Air Capture Plants. *J. Clean. Prod.* **2019,** *224*, 957-980.

24. Realmonte, G.; Drouet, L.; Gambhir, A.; Glynn, J.; Hawkes, A.; Köberle, A. C.; Tavoni, M., An Inter-Model Assessment of the Role of Direct Air Capture in Deep Mitigation Pathways. *Nat. Commun.* **2019,** *10* (1), 3277.

25. Smith, W. A.; Burdyny, T.; Vermaas, D. A.; Geerlings, H., Pathways to Industrial-Scale Fuel Out of Thin Air from CO_2 Electrolysis. *Joule* **2019,** *3* (8), 1822-1834.

26. Goeppert, A.; Meth, S.; Prakash, G. K. S.; Olah, G. A., Nanostructured Silica as a Support for Regenerable High-Capacity Organoamine-Based CO_2 Sorbents. *Energ. Environ. Sci.* **2010,** *3* (12), 1949-1960.

27. Goeppert, A.; Zhang, H.; Czaun, M.; May, R. B.; Prakash, G. K. S.; Olah, G. A.; Narayanan, S. R., Easily Regenerable Solid Adsorbents Based on Polyamines for Carbon Dioxide Capture from the Air. *ChemSusChem* **2014,** *7* (5), 1386-1397.

28. Choi, S.; Gray, M. L.; Jones, C. W., Amine-Tethered Solid Adsorbents Coupling High Adsorption Capacity and Regenerability for CO_2 Capture From Ambient Air. *ChemSusChem* **2011,** *4* (5), 628-635.

29. Goeppert, A.; Czaun, M.; May, R. B.; Prakash, G. K. S.; Olah, G. A.; Narayanan, S. R., Carbon Dioxide Capture from the Air Using a Polyamine Based Regenerable Solid Adsorbent. *J. Am. Chem. Soc.* **2011,** *133* (50), 20164-20167.

30. Kuwahara, Y.; Kang, D.-Y.; Copeland, J. R.; Brunelli, N. A.; Didas, S. A.; Bollini, P.; Sievers, C.; Kamegawa, T.; Yamashita, H.; Jones, C. W., Dramatic Enhancement of CO_2 Uptake by Poly(ethyleneimine) Using Zirconosilicate Supports. *J. Am. Chem. Soc.* **2012,** *134* (26), 10757-10760.

31. Kuwahara, Y.; Kang, D.-Y.; Copeland, J. R.; Bollini, P.; Sievers, C.; Kamegawa, T.; Yamashita, H.; Jones, C. W., Enhanced CO_2 Adsorption over Polymeric Amines Supported on Heteroatom-Incorporated SBA-15 Silica: Impact of Heteroatom Type and Loading on Sorbent Structure and Adsorption Performance. *Chem.-Eur. J.* **2012,** *18* (52), 16649-16664.

32. Sakwa-Novak, M. A.; Holewinski, A.; Hoyt, C. B.; Yoo, C.-J.; Chai, S.-H.; Dai, S.; Jones, C. W., Probing the Role of Zr Addition versus Textural Properties in Enhancement of CO_2 Adsorption Performance in Silica/PEI Composite Sorbents. *Langmuir* **2015,** *31* (34), 9356-9365.

33. Holewinski, A.; Sakwa-Novak, M. A.; Jones, C. W., Linking CO_2 Sorption Performance to Polymer Morphology in Aminopolymer/Silica Composites through Neutron Scattering. *J. Am. Chem. Soc.* **2015,** *137* (36), 11749-11759.

34. Sakwa-Novak, M. A.; Tan, S.; Jones, C. W., Role of Additives in Composite PEI/Oxide CO_2 Adsorbents: Enhancement in the Amine Efficiency of Supported PEI by PEG in CO_2 Capture from Simulated Ambient Air. *Acs Appl. Mater. Inter.* **2015,** *7* (44), 24748-24759.

35. Pang, S. H.; Lee, L.-C.; Sakwa-Novak, M. A.; Lively, R. P.; Jones, C. W., Design of Aminopolymer Structure to Enhance Performance and Stability of CO_2 Sorbents: Poly(propylenimine) vs Poly(ethylenimine). *J. Am. Chem. Soc.* **2017,** *139* (10), 3627-3630.
36. Sayari, A.; Liu, Q.; Mishra, P., Enhanced Adsorption Efficiency through Materials Design for Direct Air Capture over Supported Polyethylenimine. *ChemSusChem* **2016,** *9* (19), 2796-2803.
37. Wijesiri, R. P.; Knowles, G. P.; Yeasmin, H.; Hoadley, A. F. A.; Chaffee, A. L., CO_2 Capture from Air Using Pelletized Polyethylenimine Impregnated MCF Silica. *Ind. Eng. Chem. Res.* **2019,** *58* (8), 3293-3303.
38. Jahandar Lashaki, M.; Khiavi, S.; Sayari, A., Stability of Amine-Functionalized CO_2 Adsorbents: a Multifaceted Puzzle. *Chem. Soc. Rev.* **2019,** *48* (12), 3320-3405.
39. Wilfong, W. C.; Kail, B. W.; Jones, C. W.; Pacheco, C.; Gray, M. L., Spectroscopic Investigation of the Mechanisms Responsible for the Superior Stability of Hybrid Class 1/Class 2 CO_2 Sorbents: A New Class 4 Category. *Acs Appl. Mater. Inter.* **2016,** *8* (20), 12780-12791.
40. Wang, J.; Huang, H.; Wang, M.; Yao, L.; Qiao, W.; Long, D.; Ling, L., Direct Capture of Low-Concentration CO_2 on Mesoporous Carbon-Supported Solid Amine Adsorbents at Ambient Temperature. *Ind. Eng. Chem. Res.* **2015,** *54* (19), 5319-5327.
41. Sakwa-Novak, M. A.; Jones, C. W., Steam Induced Structural Changes of a Poly(ethylenimine) Impregnated γ-Alumina Sorbent for CO_2 Extraction from Ambient Air. *Acs Appl. Mater. Inter.* **2014,** *6* (12), 9245-9255.
42. Sakwa-Novak, M. A.; Yoo, C.-J.; Tan, S.; Rashidi, F.; Jones, C. W., Poly(ethylenimine)-Functionalized Monolithic Alumina Honeycomb Adsorbents for CO_2 Capture from Air. *ChemSusChem* **2016,** *9* (14), 1859-1868.
43. Wang, Q.; O'Hare, D., Large-Scale Synthesis of Highly Dispersed Layered Double Hydroxide Powders Containing Delaminated Single Layer Nanosheets. *Chem. Commun.* **2013,** *49* (56), 6301-6303.
44. Chen, C. P.; Yang, M. S.; Wang, Q.; Buffet, J. C.; O'Hare, D., Synthesis and Characterisation of Aqueous Miscible Organic-Layered Double Hydroxides. *J. Mater. Chem. A.* **2014,** *2* (36), 15102-15110.
45. Yu, J.; Wang, Q.; O'Hare, D.; Sun, L., Preparation of Two Dimensional Layered Double Hydroxide Nanosheets and Their Applications. *Chem. Soc. Rev.* **2017,** *46* (19), 5950-5974.
46. Yang, W. S.; Kim, Y.; Liu, P. K. T.; Sahimi, M.; Tsotsis, T. T., A Study by in Situ Techniques of the Thermal Evolution of the Structure of a Mg-Al-CO_3 Layered Double Hydroxide. *Chem. Eng. Sci.* **2002,** *57* (15), 2945-2953.
47. Zhu, X.; Chen, C.; Suo, H.; Wang, Q.; Shi, Y.; O'Hare, D.; Cai, N., Synthesis of Elevated Temperature CO_2 Adsorbents from Aqueous Miscible Organic-Layered Double Hydroxides. *Energy* **2019,** *167*, 960-969.
48. Gargiulo, N.; Peluso, A.; Aprea, P.; Pepe, F.; Caputo, D., CO_2 Adsorption on Polyethylenimine-Functionalized SBA-15 Mesoporous Silica: Isotherms and Modeling. *J. Chem. Eng. Data* **2014,** *59* (3), 896-902.
49. Gao, Y.; Zhang, Z.; Wu, J.; Yi, X.; Zheng, A.; Umar, A.; O'Hare, D.; Wang, Q., Comprehensive Investigation of CO_2 Adsorption on Mg-Al-CO_3 LDH-Derived Mixed Mental Oxides. *J. Mater. Chem. A.* **2013,** *1* (41), 12782-12790.
50. Zhao, Y.; Chen, G.; Bian, T.; Zhou, C.; Waterhouse, G.; Wu, L.; Tung, C.; Smith, L.; O'Hare, D.; Zhang, T., Defect-Rich Ultrathin ZnAl-Layered Double Hydroxide Nanosheets for Efficient Photoreduction of CO_2 to CO with Water. *Adv. Mater.* **2015,** *27* (47), 7824-7831.
51. Heydari-Gorji, A.; Sayari, A., Thermal, Oxidative, and CO_2-Induced Degradation of Supported

535 Polyethylenimine Adsorbents. *Ind. Eng. Chem. Res.* **2012,** *51* (19), 6887-6894.